

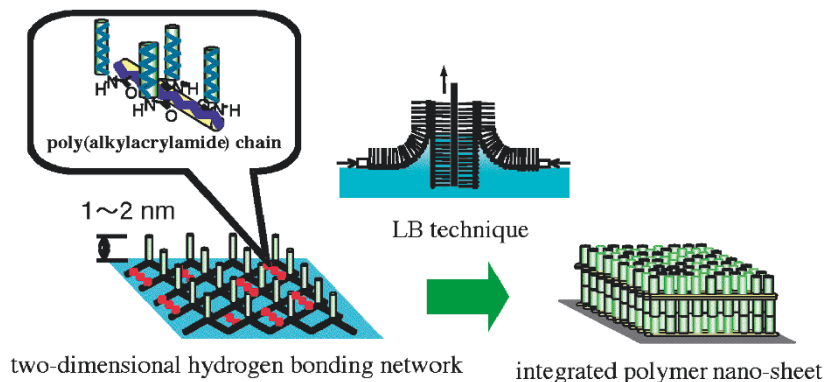
Functional Organized Molecular Assemblies Based on Polymer Nano-sheets

M. MITSUISHI, J. MATSUI,
and T. MIYASHITA

[Review Article]

Vol. 38, No. 9, pp 877–896 (2006)

Ultrathin polymer Langmuir-Blodgett films consisting of amphiphilic poly(alkylacrylamide)s are described as polymer nano-sheets through two-dimensional hydrogen network between polymer backbones, which have been developed to assemble various functional molecules and nanomaterials such as metal and magnetic nanoparticles. Surface modification and nanocoating using fluorinated polymer nano-sheets in confined area are given. Multicolored patterns based on structured color and photopatterning derived from nanostructures are demonstrated. The scope of polymer nano-sheets concerning bottom-up soft nanodevice is also reviewed.



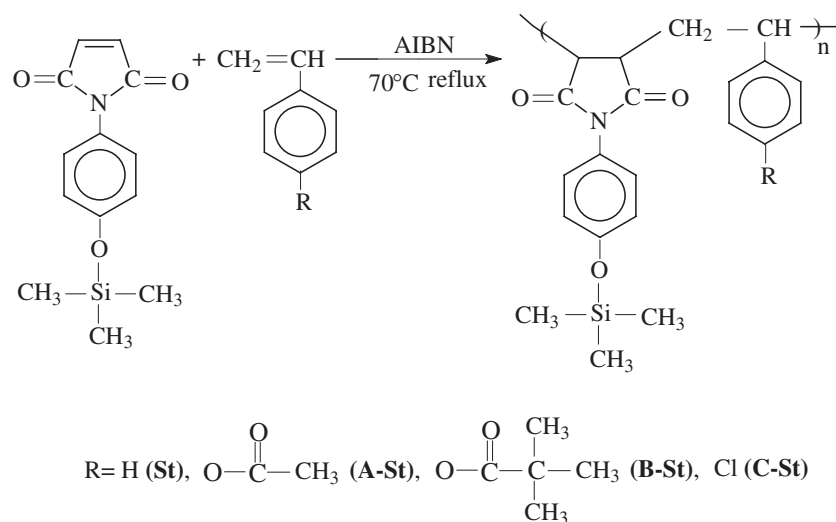
Studies of Novel Copolymers for Deep-UV Photoresists. I. Synthesis and Properties of Poly(Styrene-co-Silicon-containing maleimide)

W.-J. SHU

[Regular Article]

Vol. 38, No. 9, pp 897–904 (2006)

Soluble copolymers of trimethyl (4-(*N*-maleimido) phenoxy) silane (TMMS) with styrene-series monomers were synthesized by radical polymerization. The comonomer reactivity ratio of TMMS with styrene was changed from an alternating to middle type between alternating and ideal copolymerization. The curves of T_g s versus the different compositions of the styrene-maleimide copolymers matched the modified Johnston's equation and exhibited an S-shaped curve of deviation in comparison with the Fox's equation.



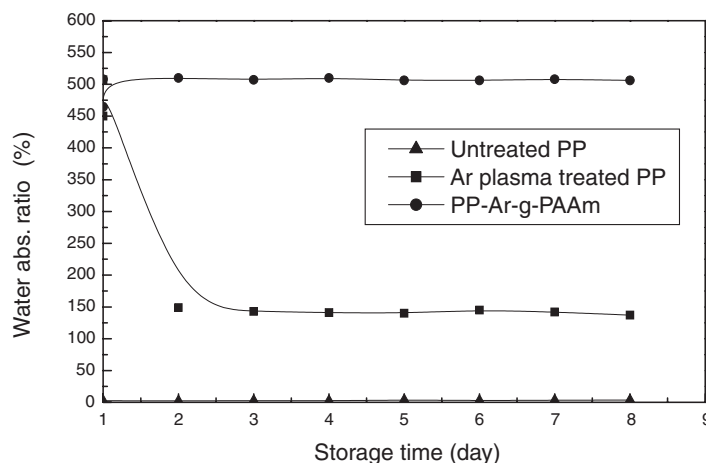
Long Term Water Adsorption Ratio Improvement of Polypropylene Fabric by Plasma Pre-treatment and Graft Polymerization

K.-S. CHEN, H.-R. LIN, S.-C. CHEN, J.-C. TSAI, and Y.-A. KU

[Regular Article]

Vol. 38, No. 9, pp 905–911 (2006)

The decrease in water absorption ratio of the only plasma-treated PP fabric can be attributed to the polar radicals generated on the surface and subsequently reacted with oxygen atoms in air to form hydrophilic functional groups on surface. However, the partial shift of polar functional groups into the inside of the film due to molecule motions would reduce the population of these hydrophilic functional groups on surface. By contrast, the monomer grafted on PP fabric was covalently permanent and can remain nearly the same hydrophilicity even after long time storage for 7 d.



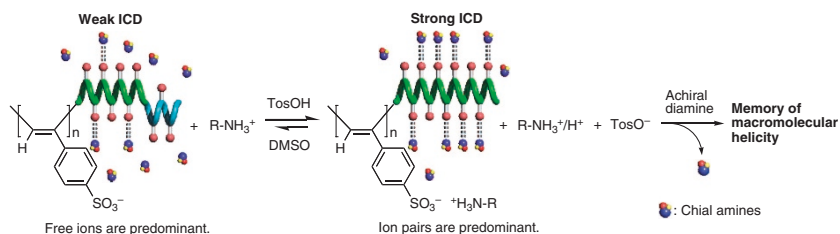
Helicity Induction on a Poly(phenylacetylene) Derivative Bearing a Sulfonic Acid Pendant with Chiral Amines and Memory of the Macromolecular Helicity in Dimethyl Sulfoxide

T. HASEGAWA, K. MAEDA, H. ISHIGURO, and E. YASHIMA

[Regular Article]

Vol. 38, No. 9, pp 912–919 (2006)

A stereoregular poly(phenylacetylene) bearing a sulfonic acid pendant (poly-1) was found to form a predominantly one-handed helix upon complexation with chiral amines in DMSO. The macromolecular helicity of poly-1 could be memorized by replacing the chiral amines with an achiral diamine. In sharp contrast to the analogous helicity induction and memory for poly(phenylacetylene)s bearing carboxy and phosphonic acid residues as the pendants, the presence of the common salt of the chiral amines was required for the effective helicity induction and subsequent memory of poly-1.



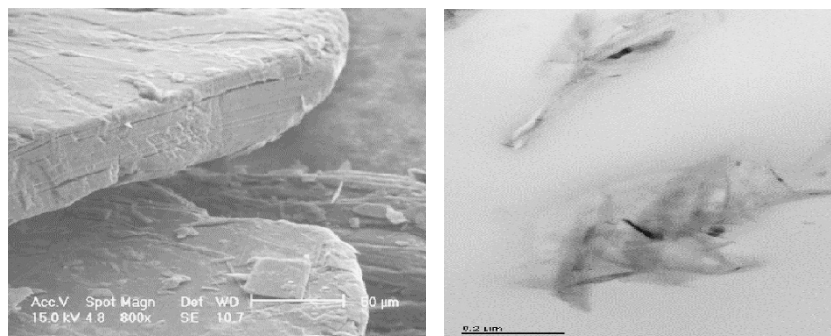
Properties and Crystallization of Maleated Polypropylene/Graphite Flake Nanocomposites

D. J. Y. S. PAGÉ and T. G. GOPAKUMAR

[Regular Article]

Vol. 38, No. 9, pp 920–929 (2006)

Polypropylene (PP)/graphite (G) hybrid nanocomposites have been prepared by melt mixing using maleated PP (PP-g-MA) and graphite oxide (GO) as compatibilizing agents. Melt mixing was achieved using a Gelimat, a high-speed thermo-kinetic mixer. The PP-g-MA and GO used as compatibilizers helped the dispersion of the graphite on a nano-scale and improved flexural properties but more significantly the impact strength of the material. TEM micrographs showed a partial exfoliation of the graphite in the PP/PP-g-MA/GO/G hybrid nanocomposites.



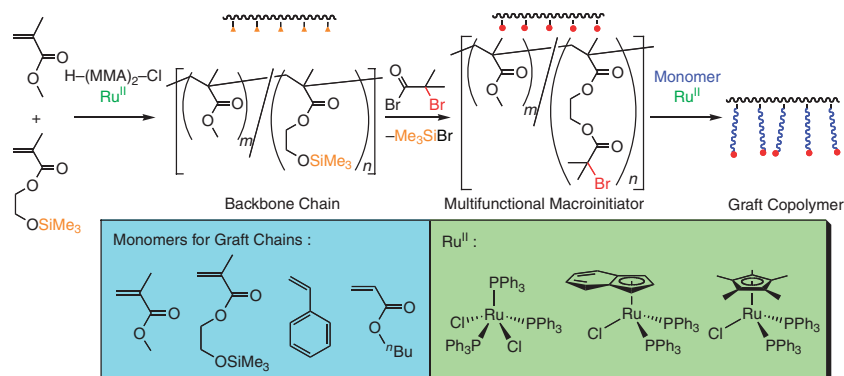
Well-Defined Graft Copolymers of Methacrylate, Acrylate, and Styrene via Ruthenium-Catalyzed Living Radical Polymerization

Y. MIURA, K. SATOH, M. KAMIGAITO, and Y. OKAMOTO

[Regular Article]

Vol. 38, No. 9, pp 930–939 (2006)

Ruthenium-catalyzed living radical polymerization was first applied to the synthesis of a series of the well-defined graft polymers. The backbone polymer was first synthesized by the living radical copolymerization of methyl methacrylate and 2-(trimethylsilyloxy)ethyl methacrylate followed by the *in situ* transformation of the silyloxy group into the ester with a C–Br bond. The obtained multifunctional macroinitiator was employed for the ruthenium-catalyzed “grafting-from” radical polymerization of methacrylate, acrylate, and styrene to afford a series of the graft polymers with controlled lengths of the backbone and graft chains.



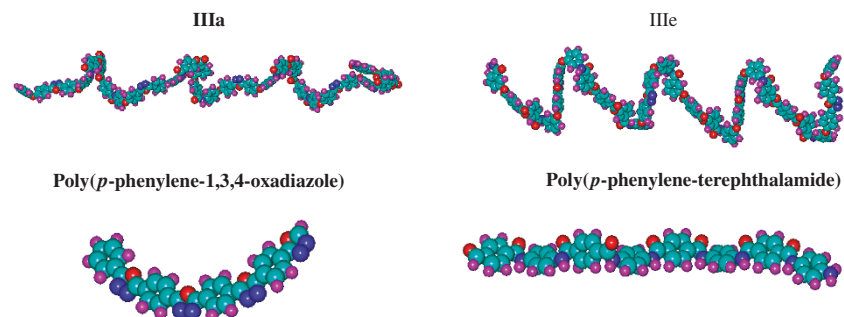
Synthesis of Poly(1,3,4-oxadiazole-amide-ester)s and Study of the Influence of Conformational Parameters on their Physical Properties

I. SAVA, I. RONOVA, and M. BRUMA

[Regular Article]

Vol. 38, No. 9, pp 940–948 (2006)

Aromatic poly(1,3,4-oxadiazole-amide-ester)s have been synthesized by reaction of aromatic diamines containing 1,3,4-oxadiazole rings with diacid chlorides containing preformed ester linkages. The polymers showed high thermal stability with decomposition temperature above 365 °C, glass transition temperature in the range 215–260 °C and good solubility. The polymer films showed tensile strength in the range 40–91 MPa, elastic modulus of 2.22–3.98 GPa and elongation at break of 1.85–7.37%. Conformational parameters of polymers have been calculated by Monte Carlo method and discussed in relation with some physical properties.



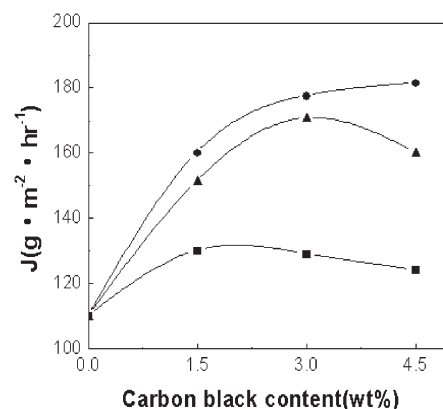
A Novel Carbon Black/Polydimethylsiloxane Composite Membrane with High Flux for the Separation of Ethanol from Water by Pervaporation

S. SHI, Z. DU, H. YE, C. ZHANG, and H. LI

[Regular Article]

Vol. 38, No. 9, pp 949–955 (2006)

A novel inorganic/organic composite membrane was prepared through introducing carbon black into PDMS membrane. The purpose to add CB to PDMS membranes was to improve the selectivity and permeation rate. The pervaporation performance of the membrane in the extraction of ethanol from ethanol/water mixtures was investigated. In certain ranges of composition, the flux simultaneously increased while the selectivity nearly had no change.



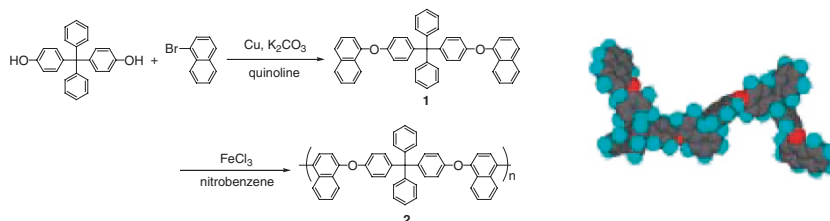
Synthesis of Poly(naphthylene ether) Containing Tetraphenylmethane Group with a Low Dielectric Constant

K. TSUCHIYA and M. UEDA

[Regular Article]

Vol. 38, No. 9, pp 956–960 (2006)

A novel thermally stable and low dielectric poly[4,4'-bis(1-naphthoxy)tetraphenylmethane] (2) has been successfully prepared. 4,4'-Bis(1-naphthoxy)tetraphenylmethane (1) as a monomer was synthesized by the Ullmann reaction from 4,4'-dihydroxytetraphenylmethane and 1-bromonaphthalene. The dielectric constants (ϵ) of polymer 2 estimated from the refractive index and the capacitance were 2.69 and 2.75, respectively.



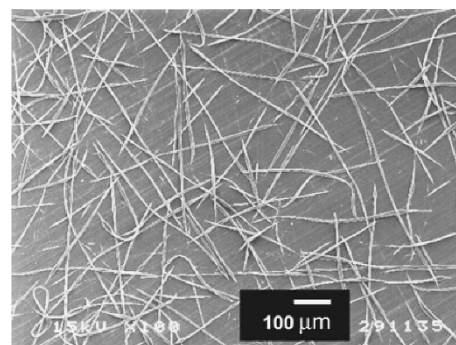
Electrospinning of Styrene-Isoprene Copolymeric Thermoplastic Elastomers

S. CHUANGCHOTE, A. SIRIVAT, and P. SUPAPHOL

[Regular Article]

Vol. 38, No. 9, pp 961–969 (2006)

SEM image of the as-electrospun product from 20% w/v solution of linear poly(styrene-*b*-isoprene-*b*-styrene) (PS-PI-PS) ($M_w \approx 140,000$ g/mol) in 1,2-dichloroethane under the applied electrical potential of 7.5 kV over a collection distance of 10 cm and the feed flow rate of 3 mL/h.



Creep Behavior of Poly(*N*-isopropylacrylamide) Gels in the Collapsed State

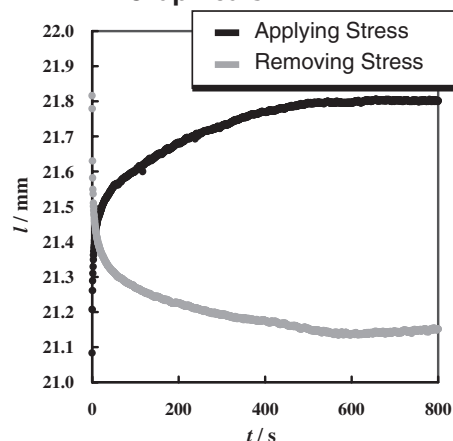
S. NOSAKA, K. URAYAMA, and T. TAKIGAWA

[Regular Article]

Vol. 38, No. 9, pp 970–975 (2006)

Creep behavior of poly(*N*-isopropylacrylamide) (PNIPA) gels in the collapsed state under static as well as dynamic stresses is investigated by using a laboratory-made magnetic force-driven rheometer. When a constant stress is applied to the cylindrical gels, the length slowly increases toward the new equilibrium value as a result of the shift to the equilibrium state under deformation. When the applied stress is removed, the length decreases with increasing time and finally reaches to the original value before deformation. These indicate that the PNIPA gels in the collapsed state undergo creep and creep recovery. The creep phenomenon is closely related to the destruction and generation of the hydrogen bonds, acting as physical crosslinks, formed in the collapsed state.

Graphicals

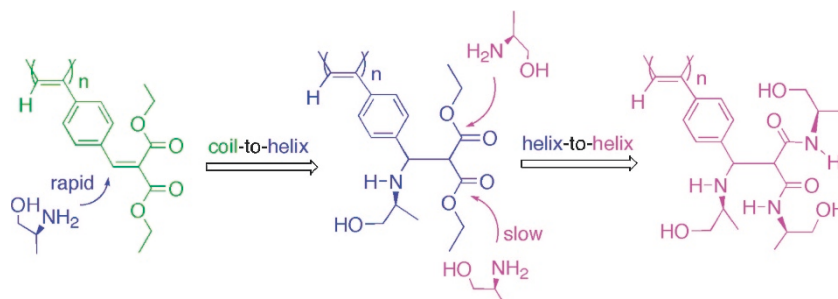


Polyacetylene Intermediate Bearing Reactive Benzylidene Malonate: Helix Induction, Inversion, and Recovery by Tandem Michael and Amidation Reactions with Chiral Nucleophiles and Water

G. KWAK, S. HOSOSHIMA, and M. FUJIKI

[Regular Article]

Vol. 38, No. 9, pp 976–982 (2006)



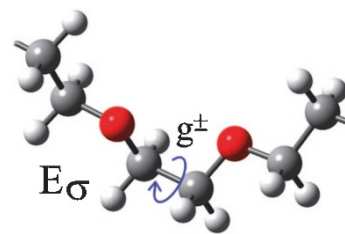
The Attractive Gauche Effect of Ethylene Oxides

Y. SASANUMA and K. SUGITA

[Regular Article]

Vol. 38, No. 9, pp 983–988 (2006)

Conformational analysis of triglyme, a trimeric model compound of poly(ethylene oxide), has been carried out. The first-order interaction energy (E_{σ}) for gauche states around the C–C bond of the terminal repeating unit is *ca.* +0.1 kcal mol⁻¹, whereas the central unit has a slightly negative E_{σ} value of *ca.* -0.1 kcal mol⁻¹. The attractive gauche effect of ethylene oxides exists independently of intramolecular (C–H)···O hydrogen bonds.



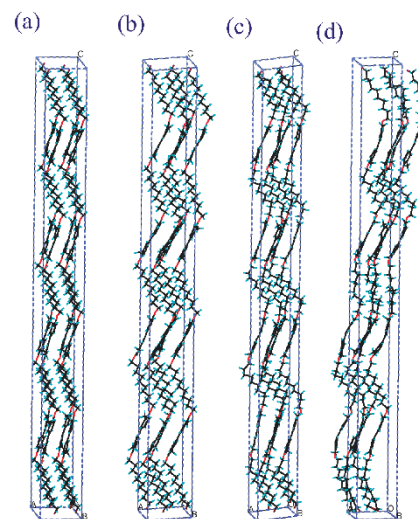
Molecular Dynamics Simulations of a Main-Chain Liquid Crystalline Polyether in the Crystalline State. 1. Chain Conformation and Dynamics of the Spacer Methylene Sequences

H. ISHIDA, Y. MAEKAWA, F. HORII, and T. YAMAMOTO

[Regular Article]

Vol. 38, No. 9, pp 989–995 (2006)

Molecular dynamics simulations have been performed for the main-chain thermotropic liquid crystalline polyether (EDMB-10), which is composed of the 3,3'-dimethyl-4,4'-biphenylene mesogens and 10-methylene spacers, in order to compare the spacer conformation and dynamics with those revealed by solid-state ¹³C NMR spectroscopy. A three-dimensional periodic cell that contains 4 or 16 short-chain molecules composed of four mesogen and five spacer units is employed, the central CH₂ sequences of the five spacer sequences being focused on for four chains in the 4-chain model or for the central four chains in the 16-chain model. At 450 K (Figure (d)), the CH₂ sequences start to adopt a conformational pair of g^+tg^- , which is frequently called the 2g1 kink, for the 4-chain model, but the introductions of the kinks are restricted to the alternate four C–C bonds. In contrast, for the 16-chain model, a pair of the g^+ and g^- conformations are allowed to introduce to the alternate four C–C bonds at almost equal probabilities without any restriction of the forms of the kinks, resulting in the good qualitative and quantitative agreements with the solid-state ¹³C NMR results.



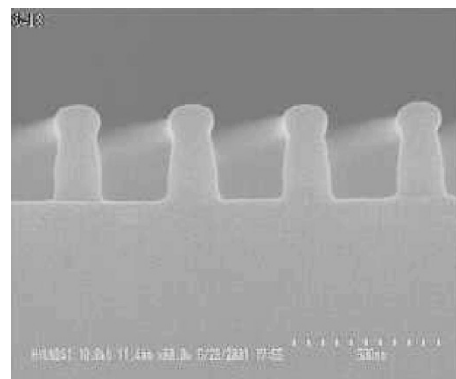
High Performance Molecular Resists Based on β -Cyclodextrin

Y. KWON, H. YUN, R. GANESAN,
J.-B. KIM, and J.-H. CHOI

[Short Communication]

Vol. 38, No. 9, pp 996–998 (2006)

Novel molecular resist based on *t*-BOC protected β -CD for deep UV lithography was synthesized and evaluated. The resist formulated with this material resolved 180 nm line patterns at a dose of 14 mJ/cm² using a KrF excimer laser lithography tool and a standard 2.38 wt% tetramethylammonium hydroxide aqueous solution. The dry-etching resistance of *t*-BOC β -CD to CF₄-reactive ion etching was comparable to that of partially *t*-BOC protected poly(4-hydroxystyrene).



Stereospecific Group Transfer Polymerization of Methyl Methacrylate with Lewis-Acid Catalysis—Formation of Highly Syndiotactic Poly(methyl methacrylate)

K. UTE, H. OHNUMA, I. SHIMIZU,
and T. KITAYAMA

[Short Communication]

Vol. 38, No. 9, pp 999–1003 (2006)

A combination of bulky aluminum bisphenoxides as the catalyst and (CH₃)₃-SiI as the co-catalyst was employed for the group transfer polymerization of MMA with ketene trimethylsilyl acetal in CH₂Cl₂. Though the whole products showed moderate syndiotacticity as well as a bimodal distribution of molecular weight (MW), the high MW fractions were found to be highly syndiotactic, whose *rr*-triad content reached 98.7% after careful fractionation by SEC.

